

Transport and Magnetic Properties of $\text{CaPd}_{3-x}\text{Cu}_x\text{O}_4$ ($x \leq 2.4$) with Interconnecting Cu(Pd)O_4 Chain Structure

Ichiro Terasaki¹, Kazuki Misawa¹, Kenji Tanabe², and Hiroki Taniguchi¹

¹Department of Physics, Nagoya University, Nagoya 464-8602, Japan

²Toyota Technological Institute, Hisakata, Tenpaku-ku, Nagoya 468-8511, Japan

We have successfully synthesized a set of polycrystalline samples of $\text{CaPd}_{3-x}\text{Cu}_x\text{O}_4$ from $x = 0$ to 2.4, and measured the resistivity, thermopower and susceptibility down to 4 K. We find that the solid solution between Pd and Cu systematically evolves the electronic ground states from a conventional band insulator to a correlated Mott insulator. In particular, $\text{CaPd}_{0.6}\text{Cu}_{2.4}\text{O}_4$ shows a magnetic phase transition at 20 K. A partial substitution of La and Y for Ca supplies electrons to $\text{CaPd}_{0.6}\text{Cu}_{2.4}\text{O}_4$, and decreases the room-temperature resistivity smaller than 10 Ωcm .

1. Introduction

Palladium oxides are known to have unique crystal structures composed of the square planar PdO_4 block.¹⁾ Above all, CaPd_3O_4 has been extensively studied owing to its peculiar properties. As shown in Fig. 1 (a), this oxide crystallizes in the cubic structure of space group $Pm\bar{3}n$ (No. 223), consisting of three PdO_4 chains intervening with each other.²⁾ The Pd ion is formally divalent, and the electronic configuration is $t_{2g}^6 d_{z^2}^2$. Accordingly, one can expect a small energy gap between d_{z^2} and $d_{x^2-y^2}$ which would vanish in a simple cubic ligand field.³⁾ Ab-initio calculations indicate an almost zero energy gap,^{4,5)} and a possibility of excitonic insulator is proposed.⁶⁾ In the presence of spin-orbit interaction, a possibility of topological insulator has been also suggested recently.⁷⁾

Another characteristic feature of CaPd_3O_4 is that electrons and holes can be doped with partial substitution of aliovalent ions for Ca. Itoh et al.^{8,9)} found that the Na substitution for Ca can supply holes to make this oxide metallic. Ichikawa and Terasaki¹⁰⁾ discussed the thermoelectric properties of $(\text{Ca}, \text{Li})\text{Pd}_3\text{O}_4$. Terasaki et al.¹¹⁾ further found that substitution of Bi for Ca can supply electrons to make this oxide n-type. Later Ozawa et al.¹²⁾ found that the isostructural oxide SrPd_3O_4 can also be n-type and p-type by substituting Bi and Na for Sr, respectively. These studies reveal that CaPd_3O_4 is a narrow-gap semiconductor, where a rigid band picture is qualitatively valid. Very recently Lamontagne et al.⁵⁾ reported that structural inhomogeneity affects the transport properties of SrPd_3O_4 and CaPd_3O_4 .

To make full use of this unique structure, we have tried to find isostructural oxide by substituting 3d transition metal ions for Pd. Eventually we have successfully synthesized the related oxide $\text{CaPd}_{0.6}\text{Cu}_{2.4}\text{O}_3$. Although this oxide still contains 20% Pd ions in the Cu site, one can extrapolate this oxide to CaCu_3O_4 that has never been synthesized.¹³⁾ In this paper, we present the sample preparation, sample characterization and physical-property measurements for $\text{CaPd}_{3-x}\text{Cu}_x\text{O}_4$, and discuss the electronic states of CaCu_3O_4 .

2. Experimental

Polycrystalline samples of $\text{CaPd}_{3-x}\text{Cu}_x\text{O}_4$ ($x = 0, 0.3, 0.6, 0.9, 1.2, 1.5, 1.8, 2.1, \text{ and } 2.4$) and $\text{Ca}_{1-y}\text{M}_y\text{Pd}_{0.6}\text{Cu}_{2.4}\text{O}_4$ ($M = \text{La and Y}; y = 0.1 \text{ and } 0.2$) were synthesized with a NaCl-flux assisted solid-state reaction.¹⁰⁾ A stoichiomet-

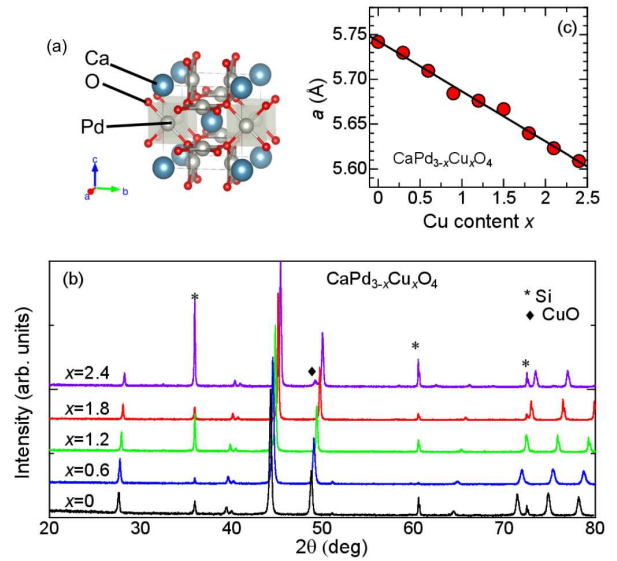


Fig. 1. (Color online) (a) The crystal structure of CaPd_3O_4 . (b) The x-ray diffraction patterns of $\text{CaPd}_{3-x}\text{Cu}_x\text{O}_4$. The Fe K_α was used as an x-ray source. For the check of the diffraction optic system, Si powder was added to the sample powder. (c) The lattice parameter plotted as a function of the Cu content x .

ric amount of CaCO_3 , PdO , CuO , La_2O_3 , Y_2O_3 powders of 99.9% purity was mixed and ground in an agate mortar. NaCl powder of 99% purity in twice weight of the sample powder was then added, and was further ground and mixed for 30 min. The powder was placed into an alumina crucible, and was heated at 800°C for 24 h in air. The added NaCl powder did not melt, but seemed to accelerate the solid-state reaction. This was effective to prevent from reducing Pd^{2+} . The heated powder was rinsed with distilled water to remove NaCl, and dried on filter paper in air at room temperature. The dried powder was pressed into pellets, and sintered at 950°C for 48 h in air. The values of x and y were taken as starting compositions of the original powders, because the cations were unlikely to evaporate at the low sintering temperature of 800°C. The x-ray diffraction except for $x = 2.4$ showed no trace of impurity phases (see later).

X-ray diffraction patterns were taken with a commercial diffractometer (Rigaku RINT2000) with a Fe K_α (1.9360Å)

used as an x-ray source in $\theta - 2\theta$ scan mode. Si powder was added to the sample powder to check the diffraction optic system. The x-ray diffraction patterns were essentially identical before and after sintering. This means that the phase of $\text{CaPd}_{3-x}\text{Cu}_x\text{O}_4$ was stable around 950°C once this phase was formed.

Resistivity was measured with a home-made measurement station from 4.2 to 300 K in a liquid He cryostat using a standard four probe method. The sample with a typical dimension of $4\times 1\times 0.5\text{ mm}^3$ was placed on a epoxy substrate attached with four gold wires of $20\text{-}\mu\text{m}$ diameter with silver paint. The voltage drop was measured against an external constant current (typically $1\ \mu$ to 1 mA) using a nanovoltmeter (Agilent 34420A). The temperature was monitored with a resistance thermometer (Lakeshore CX1030). In this setup, the measurement was unreliable, when the sample resistance exceeded the whole impedance of the measurement circuit. Thus the lowest measured temperature was limited by the sample resistance.

Thermopower was measured with a home-made measurement station from 4.2 to 300 K in a liquid He cryostat using a steady-state two probe technique. The sample bridged the gap between two copper plates with silver paint (Dupont 4922N). A copper-constantan differential thermocouple was attached across the two copper plate and a resistance heater (strain gauge was used) was placed at one of the two copper plate. The whole sample mount was encapsulated in a copper tube to ensure homogeneity of the sample temperature, which was monitored by a resistance thermometer (Lakeshore CX1030) equipped on the back side of the sample mount. The temperature difference was monitored with the differential thermocouple, and the thermoelectric voltage was measured with a nanovoltmeter (Agilent 34420A). The calibration of the sample mount was done in advance with standard samples (high-temperature conductor, constantan and copper), and the contribution of the electrical leads was carefully subtracted.

Magnetic susceptibility was measured with a commercial SQUID susceptometer (Quantum Design MPMS) in field-cooling and zero-field-cooling processes. Above room temperature, the high-temperature probe was employed. The contribution of the diamagnetic susceptibility of the sample holder was carefully subtracted.

3. Results and discussion

Figure 1(b) shows typical x-ray diffraction patterns of $\text{CaPd}_{3-x}\text{Cu}_x\text{O}_4$. For $x \leq 1.8$, no reflections from impurity phases except for Si were observed, and the samples are found to be in single phase. For $x = 2.4$, however, a tiny amount of unreacted CuO was detected. Pd oxides in general are stable in oxidized conditions, and the NaCl-flux technique effectively lowered the reaction temperature to keep oxygen equilibrium at the solid-gas interface of the ceramic surface. Even after removal of NaCl flux, synthesized CaPd_3O_4 powder was stable up to 950°C . However, this chemical stability was no longer kept at $x = 2.4$. We tried various sintering conditions, but failed in improving the sample quality for $x = 2.4$. We also tried to make samples for $x > 2.4$, but the amount of CuO increased too much to ignore.

As the Cu content x increases, all the reflections of CaPd_3O_4 phase systematically shift to higher 2θ values, indicating that the lattice parameter decreases with x . This is consistent with the different ionic radii of Pd^{2+} (0.67\AA) and Cu^{2+}

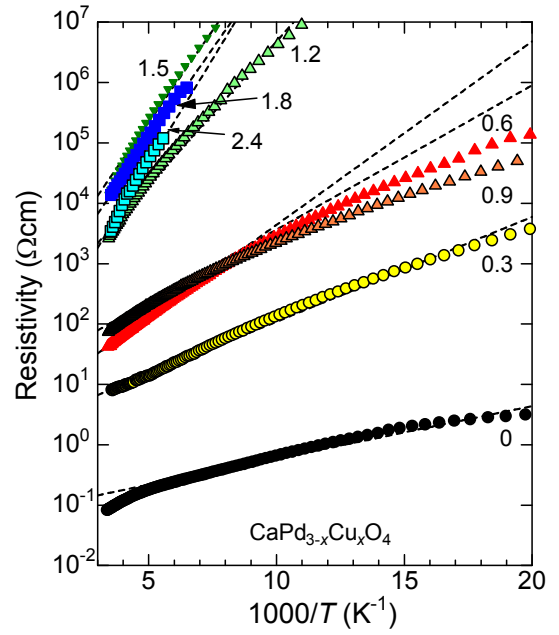


Fig. 2. (Color online) The resistivity of $\text{CaPd}_{3-x}\text{Cu}_x\text{O}_4$ plotted as a function of $1000/T$. The dotted lines represent the activation-type transport. The numbers in the figure denote the Cu content x .

(0.57\AA). Figure 1(c) indicates the lattice parameter a plotted as a function of x . Vegard's law seems valid, if $a = 5.57\text{\AA}$ is assumed for CaCu_3O_4 . Judging from the good linearity up to $x = 2.4$, we conclude that the small amount of the unreacted CuO does not seriously affect the intrinsic properties of $\text{CaPd}_{0.6}\text{Cu}_{2.4}\text{O}_3$. Aside from the lattice parameter, the relative intensity of the peaks and accordingly the crystal structure seem to be identical for all the samples. The diffraction patterns observed here are insufficient for detailed structure analysis partly owing to the small grain size of the samples caused by the NaCl-assisted growth.

Figure 2 shows the resistivity of $\text{CaPd}_{3-x}\text{Cu}_x\text{O}_4$ plotted as a function of $1000/T$ where T is the measured temperature. All the samples show non-metallic conduction, and the resistivity increases with decreasing temperature. Since all the data look linear in $1000/T$ at high temperatures, we fit the resistivity with an activation-type expression given by $\rho = \rho_0 \exp(E_g/k_B T)$ from 200 to 300 K for $x > 0$ and from 100 to 200 K for $x = 0$. The dotted lines correspond to the fitting curves, which explain the high-temperature data satisfactorily. The activation energy E_g is plotted as a function of x in Fig. 4 (see later). For example, E_g/k_B is 200 K for $x = 0$ and 1500 K for $x = 2.4$. As the Cu content x increases, the slope of the dotted curve systematically increases, and tends to saturate above $x = 1.5$. This suggests that the solid solution of $\text{CaPd}_{3-x}\text{Cu}_x\text{O}_4$ changes from one gapped state to another. This is rather unexpected, because the Cu^{2+} ion has nine d electrons, and one electron extra to the Pd^{2+} ion can contribute to conducting carriers of n-type in CaPd_3O_4 .

Let us discuss the two gapped states. Ichikawa and Terasaki analyzed the charge transport of $(\text{Ca}, \text{Li})\text{Pd}_3\text{O}_4$, and found that the activation energy of CaPd_3O_4 arises from the energy gap in the density of states (the so-called band gap). The evaluated activation energy E_g/k_B is as small as 200 K, which implies the energy difference between d_z^2 and $d_{x^2-y^2}$. Samata et

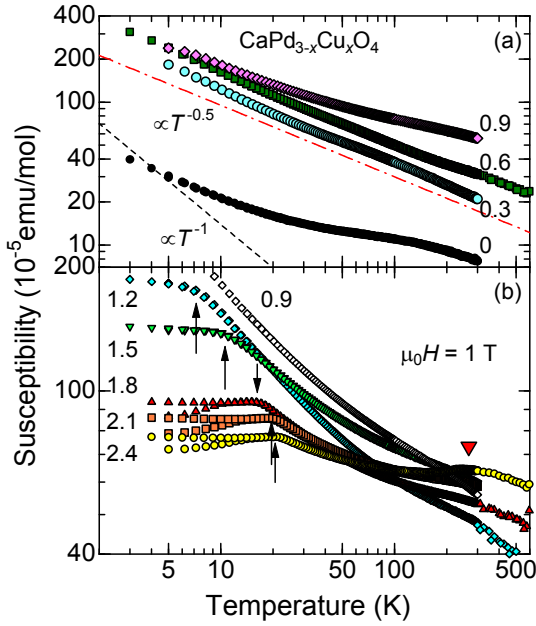


Fig. 3. (Color online) The magnetic susceptibility of $\text{CaPd}_{3-x}\text{Cu}_x\text{O}_4$ plotted as a function of temperature for (a) $x \leq 0.9$ and (b) $x \geq 0.9$. The numbers in the figure denote the Cu content x . The dotted and dot dashed lines in (a) represent $\chi \propto 1/T$ and $1/\sqrt{T}$, respectively. The arrows in (b) correspond to a magnetic phase transition temperature, and the reverse triangle in (b) indicates the broad peak for $x = 2.4$.

al.¹⁴) recently reported a similar resistivity in a single-crystal sample of $x = 0$. On the other hand, the gap for $x \geq 1.5$ comes from a different origin, because CaCu_3O_4 should be metallic (semi-metallic) from one-electron picture, as is discussed in the band calculation of Bi_2CuO_4 with the CuO_4 chain structure.¹⁵) The susceptibility data for $x = 2.4$ show an anomaly suggestive of magnetic phase transition (see below) around 20 K, and we can extrapolate that CaCu_3O_4 is a Mott insulator (magnetic insulator). Thus the gap observed in the resistivity should be associated with the Mott gap or the charge-transfer gap.¹⁶)

Figure 3 shows the magnetic susceptibility χ plotted as a function of temperature in log–log scale. As shown in Fig. 3(a), the $x = 0$ sample shows a small value of 10^{-5} emu/mol at room temperature, and increases gradually with decreasing temperature. The dotted line corresponds to the Curie law of $\chi \propto T^{-1}$, and one can find that the temperature dependence is milder than the Curie law. If we employ a phenomenological expression of $\chi \propto T^{-\gamma}$ for $x = 0$, we estimate the exponent γ to be 0.5 below 10 K (Compare the dot dashed line in Fig. 3(a)). Essentially the same temperature dependence is observed in $x = 0.3$ and 0.6, and the substituted Cu^{2+} ion seems to enhance the susceptibility of the host. We fit the susceptibility for $x = 0.6$ with the Curie–Weiss law of $C/(T+\theta_w)$, but found an unphysically large value of $\theta_w \sim 400$ K. These results clearly indicate that Cu^{2+} ions do not behave as an independent local moment of $S = 1/2$. Kanazawa and Tsuda¹⁷) measured the resistivity of $\text{Ca}_{0.7}\text{Na}_{0.3}\text{Pd}_{2.5}\text{Cu}_{0.5}\text{O}_4$. They found logarithmic temperature dependence at low temperatures, and discussed a possibility of the Kondo effect. Although they did not show the susceptibility data, their argument is consistent with the present study in the sense that the doped Cu^{2+} does not work as a simple localized moment. We

do not understand the origin for $\chi \propto T^{-\gamma}$ at present, and would like to just point out that a similar susceptibility is reported in P doped Si (Si:P) near the metal-insulator transition.¹⁸) We should also note that we prepared polycrystalline samples of $\text{SrPd}_{3-x}\text{Cu}_x\text{O}_4$ ($x = 0, 0.3$ and 0.6), and that we found their susceptibility to be essentially identical (not shown). The power-law susceptibility of $\chi \propto T^{-\gamma}$ thus characterizes the band insulator side of MPd_3O_4 ($M = \text{Ca}$ and Sr).

As shown in Fig. 3 (b), the susceptibility systematically increases with x at room temperature for $x \geq 1.2$, and shows weak temperature dependence. At low temperatures, the susceptibility shows a kink or cusp as indicated by the arrows in Fig. 3(b). This is a sign for magnetic phase transition, and thus we regard the ground state for $x \geq 1.2$ as the Mott insulator. At the present stage, the nature of the magnetic transition is yet to be explored. Below the transition temperature, the samples of $x = 1.8, 2.1$ and 2.4 show temperature hysteresis between the field-cooling and zero-field-cooling processes, suggestive of glassy nature. Considering that the degree of the hysteresis is too tiny to be identified as intrinsic, we speculate that a kind of antiferromagnetic order is realized, which should be verified with neutron diffraction.

For the $x = 2.4$ sample, one can see a broad peak around $T_{\text{peak}} = 230$ K, as indicated by the reverse triangle in Fig. 3 (b). A similar broad peak is observed in high temperature superconductors (HTSC), being interpreted as $J \sim k_B T_{\text{peak}}$ where J is the antiferromagnetic interaction.¹⁹) In low-dimensional antiferromagnetic materials with small spins, quantum fluctuation suppresses a long-range magnetic order, and induces short-range antiferromagnetic correlation. When $J > k_B T$, the $S = 1/2$ spin in the Cu^{2+} ion starts to form a local singlet with a neighbouring Cu^{2+} ion, and the susceptibility starts to decrease as the singlet correlation grows with decreasing temperature. In contrast, when $J < k_B T$, thermal fluctuation dominates to make the susceptibility be Curie–Weiss-like. Consequently, the susceptibility shows a broad peak at around $T \sim J/k_B$. If we apply this scenario to the present oxide, the interaction J is around 230 K, five times smaller than J of HTSC.^{20,21}) The ratio of the transition temperature (T_N) to J will give a rough estimate of the degree of frustration. $k_B T_N/J$ is estimated to be 0.1 for $x = 2.4$, and this small value indicates either of low-dimensionality, quantum spin, or disorder.

Let us discuss the magnetic interaction in CaCu_3O_4 . As shown in Fig. 1(a), the one-dimensional array of the CuO_4 plaquette is the basic structure responsible for magnetism. A similar CuO_4 chain is seen in Bi_2CuO_4 that exhibits an antiferromagnetic order below 50 K. In Bi_2CuO_4 , various values of the exchange interaction have been proposed.^{22–24}) Janson et al.¹⁵) calculated the magnetic interaction based on the ab-initio calculation, and found the next nearest interaction $J_2/k_B = 50$ K is dominant. Note that the nearest interaction along the chain direction is one-order-of-magnitude smaller, because the highest occupied orbital is $d_{x^2-y^2}$ for Cu^{2+} in Bi_2CuO_4 , and direct overlap of the wave function is small along the chain direction. We apply this conclusion to CaCu_3O_4 , and the next nearest interaction between the neighbouring corner-shared CuO_4 plaquettes is predominant to the in-chain nearest interaction. Shimizu et al.²¹) found that the exchange interaction is determined by the angle of the Cu–O–Cu bond. An estimated angle of 120° gives $J/k_B \sim 300$ K

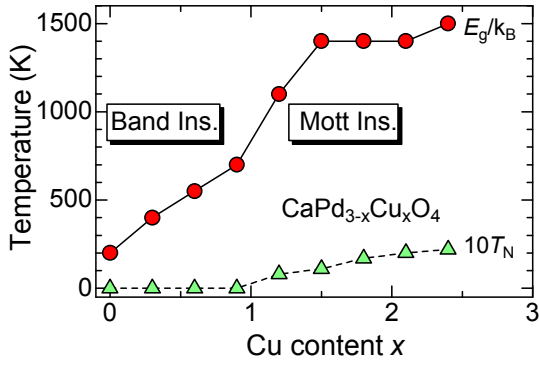


Fig. 4. (Color online) Phase diagram of $\text{CaPd}_{3-x}\text{Cu}_x\text{O}_4$. E_g is the energy gap evaluated from the activation transport in the resistivity. T_N (multiplied by 10) is the magnetic transition temperature.

for CaCu_3O_4 , which is semi-quantitatively consistent with the broad peak near 230 K for $x = 2.4$.

Figure 4 summarizes the phase diagram of the present system. The energy gap E_g/k_B evaluated from the temperature dependence of the resistivity monotonically increases from 200 K with the Cu content x up to $x = 1.5$, and stays at a constant value around 1400 K above $x = 1.5$. Concomitantly, the magnetic phase transition shows up above $x = 1.2$. This indicates that the ground state evolves from a nonmagnetic insulator to an antiferromagnetic insulator. Taking the physical properties of other Cu^{20,25} and Pd oxides^{3,26} into account, we conclude that the narrow-gap band insulator CaPd_3O_4 gradually changes to the Mott insulator $\text{CaPd}_{0.6}\text{Cu}_{2.4}\text{O}_4$ characterized by the interaction $J/k_B = 230$ K.

The new Mott insulator $\text{CaPd}_{0.6}\text{Cu}_{2.4}\text{O}_4$ could be an approximate material for CaCu_3O_4 . Let us discuss the electronic states of CaCu_3O_4 . First, it has a corner-shared CuO_4 network with the antiferromagnetic interaction of $J/k_B \sim 230$ K. Second, the CuO_4 network extends in a three-dimensional manner, and will have a dispersive conduction band as expected from the calculations of CaPd_3O_4 .³⁻⁶ On the basis of the collective wisdom of crystal chemistry of HTSC,^{27,28} we expect electrons to be doped with partial substitution of proper cations, and also expect that superconductivity may occur below around $0.1J/k_B \sim 20$ K.

In order to examine such a possibility we tried to dope electrons by partially substituting trivalent ion for Ca. Figure 5 shows the resistivity and thermopower of $\text{Ca}_{1-y}\text{M}_y\text{Pd}_{0.6}\text{Cu}_{2.4}\text{O}_3$ ($M = \text{Y}$ and La). The resistivity decreases with y , and simultaneously the thermopower changes its sign from positive to negative from $y = 0$ to 0.1, and decreases its magnitude from 0.1 to 0.2. These results strongly indicate that the majority carriers are electrons, and the partially substituted Y and La ions work as donors to supply electrons in the system. For $M = \text{Y}$, the thermopower seems saturated between $y = 0.1$ and 0.2, because a tiny amount of impurity phase of $\text{Ca}_2\text{Y}_2\text{Cu}_5\text{O}_{10}$ was detected in the x-ray diffraction pattern for $y = 0.2$.

The temperature-independent thermopower has been analyzed with the Heikes formula.²⁹ If we employ the Heikes formula given as³⁰

$$S = \frac{k_B}{e} \ln \frac{2(1-p)}{p}, \quad (1)$$

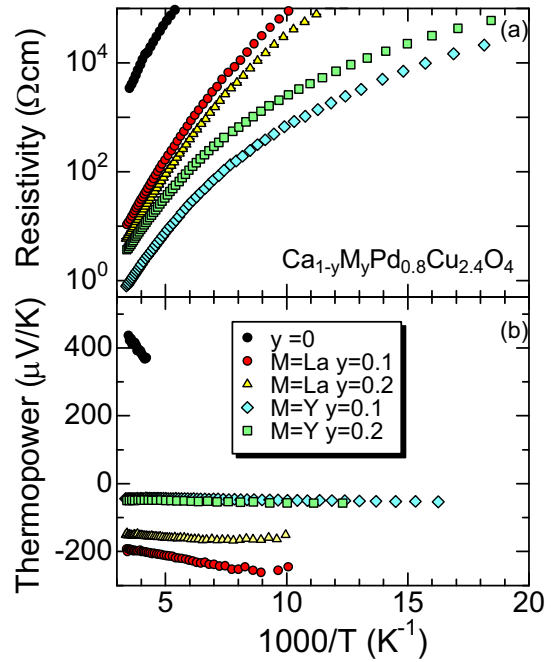


Fig. 5. (Color online) (a) Resistivity and (b) thermopower for $\text{Ca}_{1-y}\text{M}_y\text{Pd}_{0.6}\text{Cu}_{2.4}\text{O}_4$ ($M = \text{Y}$ and La) plotted as a function of $1000/T$.

where p is the electron number per site, a value of $-200 \mu\text{V/K}$ for $M = \text{La}$ and $y = 0.1$ gives $p = 0.17$ which is significantly larger than the value of $p = y/2.4 = 0.04$ expected from the chemical formula. If we took $p = 0.04$, we would have $S = -330 \mu\text{V/K}$. We do not yet understand the reason why the observed thermopower was smaller in magnitude by $130 \mu\text{V/K}$, but such small thermopowers have been often observed in the B -site disordered perovskite oxides.^{31,32} The random distribution of $4d^8$ and $3d^9$ electrons would give additional thermopower of the order of $k_B/|e| = 86 \mu\text{V/K}$,³³ which could cancel the negative thermopower. To understand the magnitude quantitatively, more systematic study is necessary.

The Heikes formula is valid when the thermal energy $k_B T$ is much larger than the transfer energy t . In reality, however, the Heikes formula unexpectedly works well for narrow-band materials even for $k_B T < t$.^{29,34} Tokura et al.²⁰ found that the magnetic interaction J is roughly equal to t^4/Δ^3 , where Δ is the charge transfer gap between Cu 3d and O 2p. If we assume the same value of Δ for all copper oxides, J is predominantly determined by t , and the small J in the present copper oxide comes from a small t , which is consistent with the non-metallic resistivity and the temperature-independent thermopower.

Unfortunately, no trace of superconductivity was observed in all the samples, perhaps because the resistivity was too high at low temperatures. In the present setup, the measurement was not accurate when the sample resistance exceeded $1 \text{ M}\Omega$. Thus we show the resistivity data below around $10^5 \Omega\text{cm}$. We tried to measure the resistance below 10 K, but observed no trace of the voltage drop. This may be due to the solid solution of Cu and Pd. If CaCu_3O_4 were synthesized, the effect of disorder would be much reduced. We also notice that $y = 0.2$ is still too small to cause superconductivity in copper oxides. According to the crystal chemistry of HTSC, superconductivity is optimized at the formal Cu valence of 1.85+ that cor-

responds to $y = 0.45$.³⁵⁾ Further improvements in the solid state chemistry are necessary to pursue superconductivity in this new copper oxide.

4. Summary

We have successfully synthesized a set of polycrystalline samples of $\text{CaPd}_{3-x}\text{Cu}_x\text{O}_4$ from $x = 0$ to 2.4, and measured the resistivity and susceptibility from 4 to 300 K. The solid solution between Pd and Cu systematically evolves the electronic states from a conventional band insulator to a correlated Mott insulator. In particular, $\text{CaPd}_{0.6}\text{Cu}_{2.4}\text{O}_4$ is successfully synthesized, suggesting a possible existence of the isostructural CaCu_3O_4 . This oxide shows a magnetic phase transition at 20 K with a broad peak around 230 K. In analogy to high-temperature superconductors, the magnetic interaction is evaluated to be around 230 K, which is 5 times smaller than that of high-temperature superconductors. A partial substitution of La and Y for Ca supplies electrons to $\text{CaPd}_{0.6}\text{Cu}_{2.4}\text{O}_4$. In the most doped sample, the room-temperature resistivity reaches smaller than $1 \Omega\text{cm}$, accompanying a small room-temperature thermopower of $-50 \mu\text{V/K}$. The conduction electrons are successfully doped, but unfortunately, no trace of superconductivity was detected in the resistivity and susceptibility measurements down to 4 K.

acknowledgement

This study was supported by a Grant-in-Aid for Scientific Research (Kakenhi No. 15K13519).

- 1) R. V. Panin, N. R. Khasanova, A. M. Abakumov, E. V. Antipov, G. V. Tendeloo, and W. Schnelle: *J. Solid State Chem.* **180** (2007) 1566.
- 2) R. C. Wnuk, T. R. Touw, and B. Post: *IBM J. Res. Dev.* **8** (1964) 185.
- 3) M. L. Doublet, E. Canadell, and M. H. Whangbo: *J. Am. Chem. Soc.* **116** (1994) 2115.
- 4) A. Khan, Z. Ali, I. Khan, S. J. Asadabadi, and I. Ahmad: *Bull. Mater. Sci.* **39** (2016) 1861.
- 5) L. K. Lamontagne, G. Laurita, M. Knight, H. Yusuf, J. Hu, R. Seshadri, and K. Page: *Inorg. Chem.* **56** (2017) 5158.
- 6) I. Hase and Y. Nishihara: *Phys. Rev. B* **62** (2000) 13426.
- 7) G. Li, B. Yan, Z. Wang, and K. Held: *Phys. Rev. B* **95** (2017) 035102.
- 8) K. Itoh, Y. Yano, and N. Tsuda: *J. Phys. Soc. Jpn.* **68** (1999) 3022.
- 9) K. Itoh and N. Tsuda: *Solid State Commun.* **109** (1999) 715.
- 10) S. Ichikawa and I. Terasaki: *Phys. Rev. B* **68** (2003) 233101.
- 11) I. Terasaki, S. Ichikawa, and S. Shibusaki: *Proc. 23rd Internat. Conf. Thermoelectrics (ICT2004)*, 2005, p. 094.
- 12) T. Ozawa, A. Matsushita, Y. Hidaka, T. Taniguchi, S. Mizusaki, Y. Nagata, Y. Noro, and H. Samata: *J. Alloys Compd.* **448** (2008) 77.
- 13) H. Müller-Buschbaum: *Angew. Chemie Internat. Ed.* **16** (1977) 674.
- 14) H. Samata, S. Tanaka, S. Mizusaki, Y. Nagata, T. Ozawa, A. Sato, and K. Kosuda: *J. Crystal. Proc. Tech.* **2** (2012) 16.
- 15) O. Janson, R. O. Kuzian, S.-L. Drechsler, and H. Rosner: *Phys. Rev. B* **76** (2007) 115119.
- 16) M. Imada, A. Fujimori, and Y. Tokura: *Rev. Mod. Phys.* **70** (1998) 1039.
- 17) M. Kanazawa and N. Tsuda: *J. Phys. Soc. Jpn.* **69** (2000) 4112.
- 18) M. P. Sarachik, A. Roy, M. Turner, M. Levy, D. He, L. L. Isaacs, and R. N. Bhatt: *Phys. Rev. B* **34** (1986) 387.
- 19) J. B. Torrance, A. Bezinge, A. I. Nazzari, T. C. Huang, S. S. P. Parkin, D. T. Keane, S. J. LaPlaca, P. M. Horn, and G. A. Held: *Phys. Rev. B* **40** (1989) 8872.
- 20) Y. Tokura, S. Koshihara, T. Arima, H. Takagi, S. Ishibashi, T. Ido, and S. Uchida: *Phys. Rev. B* **41** (1990) 11657.
- 21) T. Shimizu, T. Matsumoto, A. Goto, T. V. Chandrasekhar Rao, K. Yoshimura, and K. Kosuge: *Phys. Rev. B* **68** (2003) 224433.
- 22) J. P. Attfield: *J. Phys.: Cond. Mat.* **1** (1989) 7045.
- 23) J. L. Garcia-Munoz, J. Rodriguez-Carvajal, F. Sapina, M. J. Sanchis, R. Ibanez, and D. Beltran-Porter: *J. Phys.: Cond. Mat.* **2** (1990) 2205.
- 24) R. Troc, J. Janicki, I. Filatow, P. Fischer, and A. Murasik: *J. Phys.: Cond. Mat.* **2** (1990) 6989.
- 25) S. L. Cooper, G. A. Thomas, A. J. Millis, P. E. Sulewski, J. Orenstein, D. H. Rapkine, S.-W. Cheong, and P. L. Trevor: *Phys. Rev. B* **42** (1990) 10785.
- 26) Y. Nanao, Y. Krockenberger, A. Ikeda, Y. Taniyasu, M. Naito, and H. Yamamoto: *Phys. Rev. Materials* **2** (2018) 085003.
- 27) J. B. Torrance and R. M. Metzger: *Phys. Rev. Lett.* **63** (1989) 1515.
- 28) Y. Ohta, T. Tohyama, and S. Maekawa: *Phys. Rev. B* **43** (1991) 2968.
- 29) S. Shibusaki and I. Terasaki: *J. Phys. Soc. Jpn.* **75** (2006) 024705.
- 30) P. M. Chaikin and G. Beni: *Phys. Rev. B* **13** (1976) 647.
- 31) P. TomeÅ, J. Hejtmek, and K. KnÅek: *Solid State Sciences* **10** (2008) 486.
- 32) P. Roy, V. Waghmare, and T. Maiti: *RSC Adv.* **6** (2016) 54636.
- 33) W. Koshibae, K. Tsutsui, and S. Maekawa: *Phys. Rev. B* **62** (2000) 6869.
- 34) R. Takahashi, R. Okazaki, Y. Yasui, I. Terasaki, T. Sudayama, H. Nakao, Y. Yamasaki, J. Okamoto, Y. Murakami, and Y. Kitajima: *J. Appl. Phys.* **112** (2012) 073714.
- 35) O. Fischer, M. Kugler, I. Maggio-Aprile, C. Berthod, and C. Renner: *Rev. Mod. Phys.* **79** (2007) 353.